ADVANCED MATERIALS

Research News

Computation of Light Scattering by Anisotropic Spheres of Rutile Titania**

By Erik S. Thiele and Roger H. French*

1. Introduction

Rutile titania offers an attractive combination of physical properties that has made it the most widely used white pigment in the worldwide marketplace for coatings, plastics, and paper.[1,2] A fundamental goal of both consumers and manufacturers of rutile titania pigment is to maximize the light scattering efficiency of the pigment in end use. Achieving this goal depends upon identifying, and subsequently controlling, the factors that affect the light scattering efficiency of rutile titania powders. These factors include the particle size distribution, the degree of particle agglomeration, and the degree of optical interaction between neighboring particles in a microstructure. However, the quantitative influence of each of these factors upon the hiding power of rutile titania is not fully understood, due in large part to the difficulty of controlling laboratory experiments to the degree that the effect of each can be studied independently.[3] In the study described here, we applied a finite element method that produces rigorous full-field solutions to Maxwell's equations to the problem of light scattering by anisotropic rutile titania spheres.

Owing to the inherent experimental challenges, theoretical modeling has been used to understand light scattering properties of rutile titania. These efforts have typically relied upon Mie theory, which provides an exact treatment of the light scattering properties of a single, optically isotropic sphere.[4–6] Such studies have included investigation of the theoretical hiding power of rutile titania versus that of air voids,[7] the crowding effect in highly loaded films,[8] and the application of a multiple scattering model to predict the light scattering efficiency of paint films.[9] Mie theory has also been used to study the light scattering properties of core–shell composite particles containing inorganic coatings.[10] In reality, individual rutile titania particles exhibit both optical anisotropy and complex shapes. Mie theory is therefore not capable of rigorously describing the light scattering properties of realistic rutile titania particle shapes and microstructures. Recently, Thiele and French[11,12] have reported finite element computations on the light scattering properties of anisotropic, morphological rutile titania particles.

Attempts to use Mie theory to predict the light scattering properties of a rutile titania particle require approximation to address the optical anisotropy of the crystal. Rutile titania is uniaxial, exhibiting its ordinary refractive index for light polarized parallel to either the *a*- or *b*-axis of the crystal and its extraordinary refractive index for light polarized parallel to the *c*-axis. Two methods for approximating rutile using isotropic materials have been proposed in the literature. One approach has been to compute the mean of the refractive indices along the three crystal axes at the light wavelength of interest and subsequently apply Mie theory to compute far-field scattering parameters.[9] We refer to this as the average index approximation. Another method has been to compute separately the far-field scattering parameters for an isotropic sphere having the ordinary and extraordinary refractive indices of rutile titania, and subsequently compute the weighted sum of these separate far-field results.[7,9] The weighted sum consists of two-thirds the result for the ordinary refractive index plus one-third the result for the extraordinary refractive index. We refer to this as the weighted sum approximation.

In the present study, we employ a finite element method to compute the near- and far-field scattering properties of optically anisotropic spheres of rutile titania at the wavelength of 560 nm. These results were then compared to results obtained using Mie theory under both the average index and weighted sum approximations. The finite element method produces rigorous solutions to Maxwell's equations for electromagnetic radiation interacting with arbitrary microstructures, which can contain optically anisotropic materials. The finite element approach can therefore be used to determine the light scattering properties of realistic systems that would otherwise be inaccessible. In the case of light scattering by an optically anisotropic sphere, results obtained using the finite element method contain the effects of the optical activity of the uniaxial crystal, unlike the results of either of the two aforementioned approximations based upon scattering by isotropic spheres.

[*] Dr. R. H. French, Dr. E. S. Thiele
DuPont Central Research and Development
Experimental Station
PO Box 80356, Wilmington, DE 19880-0356 (USA)

[**] The authors thank J. Mould, Jr. for computational support in implementing the finite element code.

Elong Int'l USA Inc. - EX1014

2. Computational Approach

2.1. Finite Element Method

A review of the finite element method for the computation of electromagnetic radiation scattering is available in the literature.[13] Briefly, the method is based upon piecewise solution of the time domain form of Maxwell's equations in source-free space given in Equation 1, where the computational domain is discretized into a finite number of volume elements. Here, E is electric field amplitude, ε the electric permittivity of the medium, and μ the magnetic permeability of the medium. The finite element method is a general formulation that can be applied in diverse electromagnetic applications.[14,15]

$$\nabla^2 \boldsymbol{E} - \varepsilon\mu \frac{\partial^2 \boldsymbol{E}}{\partial t^2} = 0 \tag{1}$$

The finite element models in the present study are constructed in a Cartesian coordinate system by specifying edge dimensions, the finite element mesh density, particle position(s) and shape(s), and the optical properties of the constituent materials at the wavelength of interest. Typical models contain ~2 million elements. Electromagnetic radiation is allowed to propagate within the finite element model in the time domain, with electric field amplitude and phase computed at each node in the finite element model at each time step. A sufficient number of time steps are executed in a computation to ensure that steady state is achieved. The scattered electric field at near field is extrapolated onto the surface of a far-field sphere having a radius that is very large compared to the wavelength of the radiation. The simulation of diffuse illumination is accomplished by superimposing the far-field scattered intensities computed in a series of individual computations in which the illumination directions are varied step-wise over the necessary range of orientations.

After extrapolation of the scattered electric field and intensities has been accomplished, it is straightforward to extract macroscopically observable physical quantities such as the scattering cross section C_{sca} of the microstructure being modeled and the angular distribution of scattered light. The scattering cross section is defined in Equation 2 and is expressed in units of area, where θ is the scattering angle, I_0 the incident radiation intensity, and $I_{sca}(\theta)$ the scattered intensity on the surface of a far-field sphere over which the surface integral is performed.

$$C_{sca} = \frac{1}{I_0} \iint_{4\pi} I_{sca}(\theta) \mathrm{d}\Omega \tag{2}$$

It is instructive to normalize the scattering cross section by the volume of the scattering material in the finite element model. The scattering coefficient S is defined in Equation 3 and is expressed in dimensions of inverse length.

$$S = C_{sca}/V \tag{3}$$

The scattering coefficient S provides information about the strength of light scattering by a particular microstructure on a per-volume basis. It provides no direct information, however, about the efficiency of a microstructure in deflecting light away from the direction of incidence; in a paint film, for example, a combination of strong scattering per volume and strong deflection of light is desired, since it is this combination that imparts hiding power. The asymmetry parameter g (Eq. 4) is the average cosine of the scattering angle associated with a scattering microstructure, weighted by the scattered intensity as a function of scattering angle.

$$g = \frac{\iint_{4\pi} I(\theta) \cos\theta \, \mathrm{d}\theta}{\iint_{4\pi} I(\theta) \, \mathrm{d}\theta} \tag{4}$$

The asymmetry parameter g is dimensionless and varies between –1 (for perfect backwards scattering) and 1 (for perfect forward scattering). Both the asymmetry parameter and the scattering coefficient play prominent roles in multiple scattering theory, where the term defined here as the angle-weighted scattering coefficient σ (Eq. 5) expresses the combined ability of a scattering feature to strongly deflect incident electromagnetic radiation away from the direction of incidence.[16]

$$\sigma = S\,(1-g) \tag{5}$$

The angle-weighted scattering coefficient σ, like the scattering coefficient S, has dimensions of inverse length. It can be considered a figure of merit in the context of the ability of a scattering feature in a paint film to contribute to hiding power. Throughout this article, scattering results are expressed in terms of both the scattering coefficient S and the angle-weighted scattering coefficient σ.

2.2. Mie Theory

To quantify the accuracy of the finite element method, it is useful to compare results obtained using the finite element method for scattering by an isotropic sphere to the exact results obtained using Mie theory. To compute the Mie theory results presented below, we have employed the BHMIE computer code provided by Bohren and Huffman,[6] with additional code introduced for computation of the asymmetry parameter. In this computational approach, series expansions are performed to compute the scattering cross section and asymmetry parameter at far field.

3. Scattering by Single Anisotropic Spheres

The light scattering properties of thirteen anisotropic, high-index spheres having the optical constants of rutile titania have been computed using the finite element method. The light wavelength used in these computations is 560 nm, the center of the visible spectrum. At this wavelength, the

 © WILEY-VCH Verlag GmbH, D-69469 Weinheim, 1998 0935-9648/98/1510-1272 $ 17.50+.50/0

15214095, 1998, 15, Downloaded from https://onlinelibrary.wiley.com/doi/10.1002/(SICI)1521-4095(199801)10:15<1271::AID-ADMA1271>3.0.CO;2-C by Georgia Institute Of Technology, Wiley Online Library on [27/07/2024]. See the Terms and Conditions (https://onlinelibrary.wiley.com/terms-and-conditions) on Wiley Online Library for rules of use; OA articles are governed by the applicable Creative Commons License

ADVANCED MATERIALS

ordinary refractive index of rutile titania has been reported as 2.64, while the extraordinary index has been reported as 2.94.[17] The physical symmetry elements of an anisotropic, uniaxial sphere include an equatorial mirror plane and a cylindrical rotation axis perpendicular to this mirror plane. (In this description, the optic axis intersects the surface of the sphere at the two poles.) The complete light scattering behavior of such a system can therefore be sampled through a series of illuminations along any arc connecting one pole of the sphere to the equator. We use six different illumination directions for each sphere at the evenly spaced angles 7.5°, 22.5°, 37.5°, 52.5°, 67.5°, and 82.5° relative to the optic axis. Two mutually perpendicular polarizations (parallel and perpendicular to the optic axis of the sphere) are used for each illumination direction, resulting in a total of 12 individual illuminations per sphere. The far-field scattering parameters S and σ are computed for each sphere by computing the averages of these two quantities, weighting the individual results by the probabilities of occurrence associated with each of the illumination directions; under conditions of random illumination, illumination directions nearly perpendicular to the optic axis are more probable than those nearly parallel to the optic axis.

The finite element models for each of the spheres studied consisted of a spherical particle at the center of a cubic finite element model. In each case, the sphere is surrounded by an optically isotropic medium with refractive index $n = 1.514$, representative of an acrylic resin.[7] The finite element mesh density differs from model to model but is typically 50–60 elements per wavelength in the highest index material in the model. In the case of the 0.2 μm sphere, for example, the cubic element edge length is 3.87 nm. In general, finer finite element meshes lead to improved accuracy. Previous accuracy analysis of this finite element approach[11,12] suggests that the error associated with each of the calculations in this study should be less than 2 %.

The full near-field results of a finite element computation performed on the 0.2 μm anisotropic sphere are shown in Figure 1. The upper left panel of the figure shows a three-dimensional view of the sphere (with the surrounding

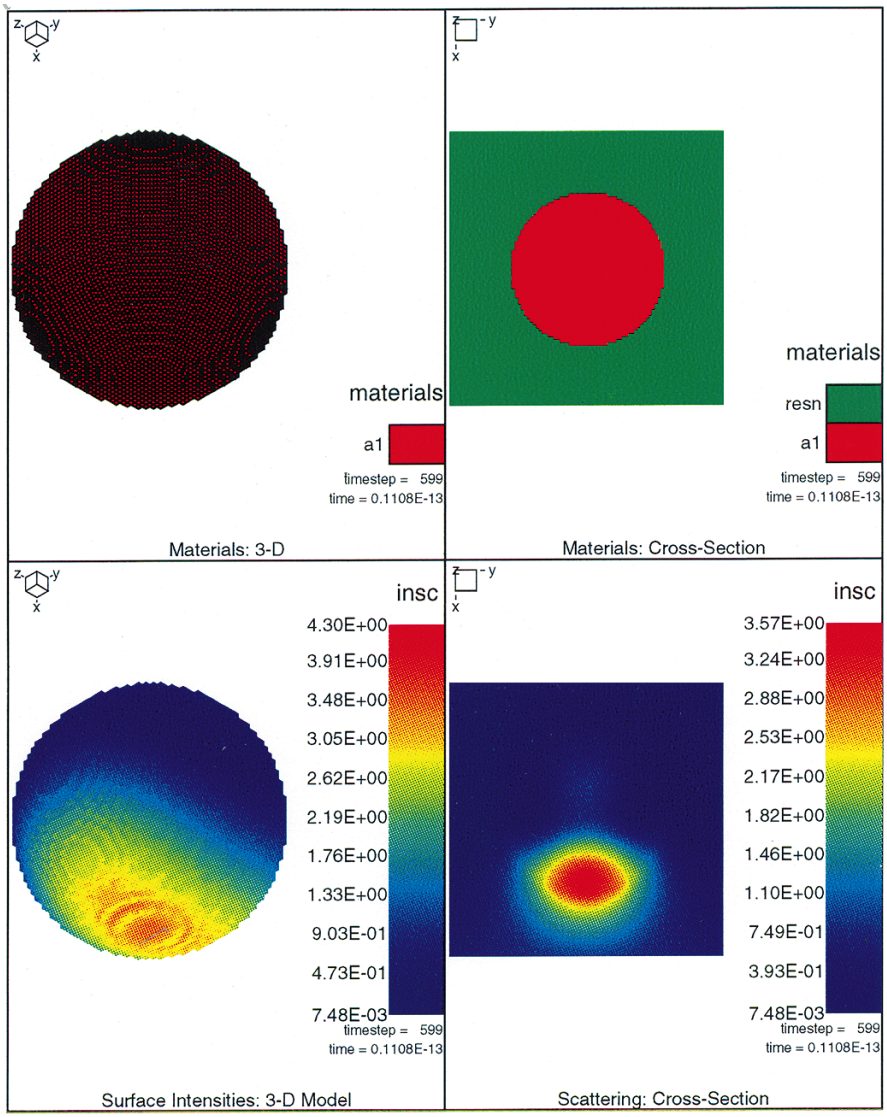

Fig. 1. Finite element model and scattered intensities for a 0.2 μm anisotropic sphere of rutile titania. The 560 nm radiation propagates in the $+x$ direction, with unit incident intensity. Polarization is parallel to the y direction.

 © WILEY-VCH Verlag GmbH, D-69469 Weinheim, 1998 0935-9648/98/1510-1273 $ 17.50+.50/0

15214095, 1998, 15, Downloaded from https://onlinelibrary.wiley.com/doi/10.1002/(SICI)1521-4095(199801)10:15<1271::AID-ADMA1271>3.0.CO;2-C by Georgia Institute Of Technology, Wiley Online Library on [27/07/2024]. See the Terms and Conditions (https://onlinelibrary.wiley.com/terms-and-conditions) on Wiley Online Library for rules of use; OA articles are governed by the applicable Creative Commons License

medium removed for clarity), and the upper right panel shows a cross-sectional view through the center of the finite element model. The lower two panels show steady-state scattered intensities in the views corresponding to the two panels above. In this computation, the 560 nm incident light propagates in the finite element model in the $+x$ direction, and the incident polarization is parallel to the y direction. The incident intensity of the light is equal to unity. In both of the lower panels of Figure 1, the scattered intensities in the model are as much as 4.3 times greater than the incident intensity. This concentration of scattered light in the vicinity of the particles is characteristic of scattering of electromagnetic radiation by highly resonant features.

Using the methodology described above, the far-field parameters S and σ have been computed for a series of anisotropic spheres of rutile titania with diameters in the range 0.05–0.35 μm. Results for the scattering coefficient S are summarized in Table 1 and plotted versus sphere diameter in Figure 2 (filled circles). These data exhibit a sharp increase in S as the sphere diameter is increased from 0.05 to 0.2 μm, beyond which resonant peaks are observed as the diameter is further increased. Results for the angle-weighted scattering coefficient σ are also summarized in Table 1 and plotted versus sphere diameter in Figure 3 (filled circles). These data exhibit the same sharp increase in σ as the sphere diameter increases from 0.05 to 0.2 μm, in a qualitative sense, as the S results in Figure 2. For sphere diameters greater than 0.2 μm, the σ data in Figure 3 decrease without the same pronounced resonant peaks observed in the S data.

Table 1. Scattering coefficients S and σ computed for anisotropic spheres of different diameter using the finite element approach.

Diameter [μm]	S [μm^{-1}]	σ [μm^{-1}]
0.050	0.587	0.564
0.100	4.52	3.79
0.150	12.50	7.03
0.175	20.06	8.82
0.187	23.94	11.73
0.200	25.62	12.34
0.212	22.27	11.30
0.225	21.01	10.37
0.250	22.17	9.41
0.275	25.83	9.68
0.300	22.10	9.07
0.325	18.89	9.43
0.350	18.91	8.44

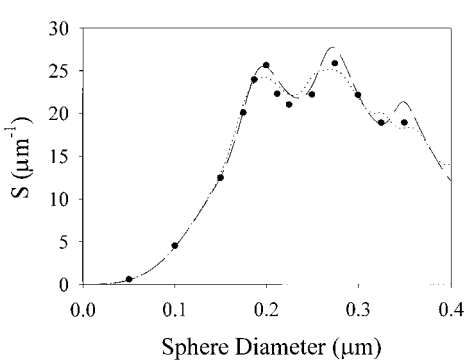

Fig. 2. The scattering coefficient S as a function of sphere diameter computed using the finite element method for anisotropic spheres of rutile titania embedded in a medium with n = 1.514 (filled circles). The illumination wavelength is 560 nm. Results using the average index approximation (dashed curve) and the weighted sum approximation (dotted curve) are shown for comparison.

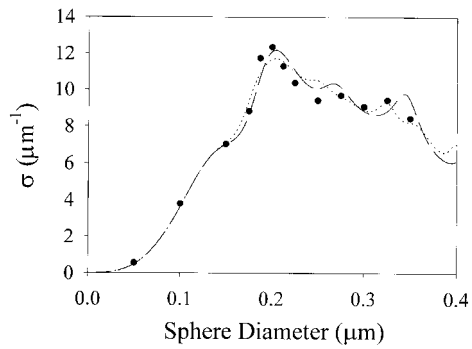

Fig. 3. The angle-weighted scattering coefficient σ as a function of sphere diameter computed using the finite element method for anisotropic spheres of rutile titania embedded in a medium with n = 1.514 (filled circles). The illumination wavelength is 560 nm. Results using the average index approximation (dashed curve) and the weighted sum approximation (dotted curve) are shown for comparison.

4. Discussion

4.1. Angle and Polarization Dependence of Scattering by an Anisotropic Sphere

An essential difference between radiation scattering by an optically anisotropic sphere versus an optically isotropic sphere is the dependence of the far-field scattering properties upon illumination direction and polarization, resulting from the optical activity of the optically anisotropic sphere. In addition, an optically anisotropic sphere exhibits polarization dependence in its far-field scattering parameters, with the exception of the special case where the incident radiation propagates parallel to the optic axis of a sphere that is uniaxial. These effects can be observed in the scattering properties of each of the anisotropic spheres studied here. The combined effects of the direction of light incidence and polarization for the case of the 0.2 μm sphere are shown in Figure 4. Plotted in this figure is the scattering coefficient S versus the angle of light incidence for polarization both parallel to (filled circles) and perpendicular to (empty circles) the sphere optic axis. The angle of incidence is defined as the angle between the propagation direction of the incident light and the optic axis of the sphere. The curves in Figure 4 converge to the same values at low angles of incidence; this is expected, since both orthogonal polarizations for light incident at low angles sample primarily the ordinary refractive index of the crystal. As the angle of incidence increases, the scattering coefficient associated with polarization parallel to the sphere optic axis increases markedly as it is exposed increasingly to the larger,

15214095, 1998, 15, Downloaded from https://onlinelibrary.wiley.com/doi/10.1002/(SICI)1521-4095(199801)10:15<1271::AID-ADMA1271>3.0.CO;2-C by Georgia Institute Of Technology, Wiley Online Library on [27/07/2024]. See the Terms and Conditions (https://onlinelibrary.wiley.com/terms-and-conditions) on Wiley Online Library for rules of use; OA articles are governed by the applicable Creative Commons License

ADVANCED MATERIALS

extraordinary index of the rutile crystal. For polarization perpendicular to the optic axis, however, no component of the incident light is exposed to the extraordinary refractive index of the crystal, resulting in no dependence of S upon the angle of incidence. In Figure 4, the scattering coefficient S for unpolarized light incident from any of the angles shown can be computed by averaging the values associated with the two orthogonal polarizations.

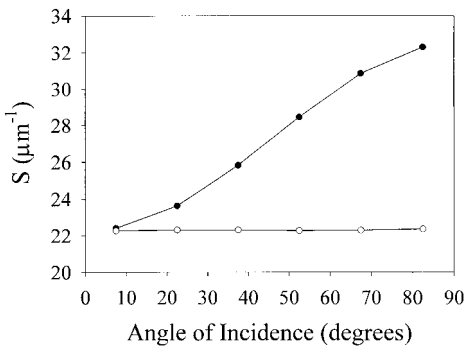

Fig. 4. Scattering coefficient S as a function of the angle of incidence of the light (relative to the optic axis) for a 0.2 μm anisotropic sphere of rutile titania. Empty circles are for polarization perpendicular to the optic axis of the sphere; filled circles are for polarization coplanar with the optic axis. These results were computed using the finite element method.

4.2. The Validity of the Average Index and Weighted Sum Approximations

A question of central interest in this study is to what degree the average index and weighted sum approximations described in Section 1 succeed in predicting the far-field scattering parameters associated with the anisotropic spheres investigated here.

The agreement in the scattering coefficient S between the results computed using the finite element method and both the average index (dashed curve) and the weighted sum (dotted curve) approximations is shown in Figure 2. In both cases, agreement between the finite element method results for anisotropic spheres and the approximate approaches is excellent for diameters 0.18 μm and smaller. The weighted sum approximation underestimates the first resonant peak in the finite element results (0.2 μm sphere), but the average index approximation accurately matches this peak value. For diameters greater than 0.2 μm, differences of up to 10 % occur between the two approximations and the finite element results. The three data sets in Figure 2 suggest that the periodicity of the resonant peaks in the finite element results is longer than in either of the two approximations. It has been suggested that such resonant peaks arise from resonant surface waves on a sphere;[5] it is therefore reasonable that the different symmetry of an anisotropic sphere compared to an isotropic should result in a quantitatively different behavior of such resonances. It is not immediately clear why the period of the resonant peaks associated with anisotropic spheres is longer than either of the two approximations based upon isotropic spheres. Comparison of the average index and weighted sum approximation data sets in Figure 2 indicate that the main difference between the two is that the resonant peaks in the weighted sum approximation are less sharp. That approximation is a weighted superposition of two curves that are slightly offset with respect to sphere diameter, resulting in averaging of the resonant peaks.

The agreement of the angle-weighted scattering coefficient σ between the finite element method and both the average index (dashed curve) and weighted sum (dotted curve) approximations is shown in Figure 3. In analogy with results for the scattering coefficient S in Figure 2, agreement between the finite element data and both approximations is very good for diameters less than 0.18 μm. For sphere diameters greater than this value, the data sets contain the same resonant features, with the period of the resonant peaks for the finite element data again being greater than that of the average index approximation. In both S and σ, the maximum values in the average index approximation (sphere diameter ~0.2 μm) are in very good agreement with the finite element data. The most significant disagreement between the weighted sum approximation and the finite element data occurs around the primary resonant peak, around 0.2 μm. The average index approximation more accurately fits this first resonant peak than the weighted sum approximation in both S and σ.

The statistical quantity χ^2 has been computed as a means of quantifying the ability of both the average index and weighted sum approximations to predict the results for S and σ of anisotropic spheres obtained using the finite element method. The complete data sets in Figures 2 and 3 were used. The quantity σ^2 has been computed using Equation 6, where n is the number of data points (thirteen, in this case), O_k is the value of S or σ computed for a given sphere diameter using either the average index or weighted sum approximations, and E_k is the value of S or σ computed for the sphere diameter using the finite element method.

$$\chi^2 = \sum_{k=1}^{n} \frac{(O_k - E_k)^2}{E_k} \tag{6}$$

The values of χ^2 computed for the average index and weighted sum approximations are summarized in Table 2 for both quantities S and σ. The value of χ^2 is significantly smaller than the number of data points for each data set, indicating a very good statistical fit in each case. For both S and σ, the weighted sum approximation exhibits slightly lower χ^2 values

Table 2. Values of χ^2 (Eq. 6) associated with S and σ values for the average index and weighted sum approximations, compared to anisotropic sphere scattering data generated using the finite element approach.

	S	σ
Average index approximation	0.71	0.44
Weighted sum approximation	0.60	0.33

 © WILEY-VCH Verlag GmbH, D-69469 Weinheim, 1998 0935-9648/98/1510-1275 $ 17.50+.50/0

15214095, 1998, 15, Downloaded from https://onlinelibrary.wiley.com/doi/10.1002/(SICI)1521-4095(199801)10:15<1271::AID-ADMA1271>3.0.CO;2-C by Georgia Institute Of Technology, Wiley Online Library on [27/07/2024]. See the Terms and Conditions (https://onlinelibrary.wiley.com/terms-and-conditions) on Wiley Online Library for rules of use; OA articles are governed by the applicable Creative Commons License

than the weighted sum approach, but this can be reversed by selectively omitting certain discrete data points from the data sets, indicating no clear advantage to either approach from a statistical standpoint.

While both the average index and weighted sum approximations are in good statistical agreement with the results of finite element computations for anisotropic spheres, there are possible advantages associated with each for a given circumstance. The average index approximation offers the advantage of explicitly defining a single refractive index for the material, therefore requiring only a single set of computations to obtain far-field results. The weighted sum approximation offers the advantage of smoothing out the sharp resonant peaks associated with particular sphere diameters in Mie theory computations, artifacts of the high symmetry of a sphere that in practice are not observed in light scattering by real systems of multiple particles.

5. Conclusions

Efforts to model the light scattering properties of rutile titania have typically relied upon Mie theory, which is limited to the description of a single, isotropic sphere. This approach requires simplifying approximations to address the optical anisotropy of the particles. In the study described here, we applied a finite element method that produces rigorous solutions to Maxwell's equations to the problem of light scattering by anisotropic rutile titania spheres. We observed resonances in the far-field scattering coefficients that depend upon sphere diameter, in analogy with approximations based on Mie theory. The far-field scattering coefficient depends upon both the angle of incidence of light and the polarization. For a 0.2 μm sphere, we observe that polarization parallel to the optic axis of the sphere results in larger scattering coefficients than the perpendicular polarization. This is consistent with the fact that the extraordinary refractive index of the crystal is greater than the ordinary at the 560 nm wavelength studied. The results of this numerical approach are compared to the two usual Mie theory approximations used to address the anisotropy of rutile titania. Both approximations are in good statistical agreement with the finite element results, although the period of the resonant peaks for anisotropic spheres is longer than in either of the approximations.

[1] J. H. Braun, A. Baidins, R. E. Marganski, *Prog. Org. Coat.* **1992**, *20,* 105.
[2] T. C. Patton, *Pigment Handbook*, Wiley, New York **1973**.
[3] D. P. Fields, R. J. Buchacek, J. G. Dickinson, *J. Oil Colour Chem. Assoc.* **1993**, *2*, 87.
[4] G. Mie, *Ann. Phys. (Leipzig)* **1908**, *25*, 377.
[5] H. C. van de Hulst, *Light Scattering by Small Particles*, Dover, New York **1981**.
[6] C. F. Bohren, D. R. Huffman, *Absorption and Scattering of Light by Small Particles*, Wiley-Interscience, New York **1983**.
[7] W. D. Ross, *J. Paint Technol.* **1971**, *43*, 50.
[8] S. Fitzwater, J. W. Hook III, *J. Coat. Technol.* **1985**, *57*, 39.
[9] B. R. Palmer, P. Stamatakis, C. F. Bohren, G. C. Salzman, *J. Coat. Technol*. **1989**, *61*, 41.
[10] R. W. Johnson, E. S. Thiele, R. H. French, *TAPPI J.* **1997**, *80*, 233.
[11] E. S. Thiele, R. H. French, *J. Am. Ceram. Soc.* **1998**, *81*, 469.
[12] E. S. Thiele, R. H. French, in *Proc. of the 4th Nürnberg Congress of the Paint Research Association*, Paint Research Association, Teddington, UK **1997**.
[13] J. L. Volakis, A. Chatterjee, L. C. Kempel, *J. Opt. Soc. Am. A* **1994**, *11*, 1422.
[14] G. L. Wojcik, J. Mould, L. West, in *Integrated Photonics Research 1993*, Technical Digest Series, Vol. 10, Optical Society of America, Washington, DC **1993**.
[15] G. L. Wojcik, D. K. Vaughan, L. K. Galbraith, *Proc. SPIE* **1987**, *774*, 21.
[16] C. F. Bohren, *Am. J. Phys.* **1987**, *55*, 524.
[17] M. W. Ribarsky, *Handbook of Optical Constants* (Ed: E. D. Palik), Academic, New York **1985**.

 © WILEY-VCH Verlag GmbH, D-69469 Weinheim, 1998 0935-9648/98/1510-1276 $ 17.50+.50/0

15214095, 1998, 15, Downloaded from https://onlinelibrary.wiley.com/doi/10.1002/(SICI)1521-4095(199808)10:15<1271::AID-ADMA1271>3.0.CO;2-C by Georgia Institute Of Technology, Wiley Online Library on [27/07/2024]. See the Terms and Conditions (https://onlinelibrary.wiley.com/terms-and-conditions) on Wiley Online Library for rules of use; OA articles are governed by the applicable Creative Commons License